ACS APPLIED MATERIALS & INTERFACES

www.acsami.org

Research Article

Field-Assisted Alignment of Cellulose Nanofibrils in a Continuous Flow-Focusing System

Heather G. Wise, Hidemasa Takana, Fumio Ohuchi, and Anthony B. Dichiara*

Cite This: *ACS Appl. Mater. Interfaces* 2020, 12, 28568−28575

Read Online

ACCESS | Metrics & More | Article Recommendations | Supporting Information

ABSTRACT: The continuous production of macroscale filaments of 17 μm in diameter comprising aligned TEMPO-oxidized cellulose nanofibrils (CNFs) is conducted using a field-assisted flow-focusing process. The effect of an AC external field on the material's structure becomes significant at a certain voltage, beyond which augmentations of the CNF orientation factor up to 16% are obtained. Results indicate that the electric field significantly contributes to improve the CNF ordering in the bulk, while the CNF alignment on the filament surface is only slightly affected by the applied voltage. X-ray diffraction shows that CNFs are densely packed anisotropically in the plane parallel to the filament axis without any preferential out of plane orientation. The improved nanoscale ordering combined with the tight CNF packing yields impressive enhancements in mechanical properties, with stiffness up to 25 GPa and more than 63% (up to 260 MPa), 46% (up to 2.8%), and 120% (up to 4.7 kJ/m^3) increase in tensile strength, strain-to-failure, and toughness, respectively. This study demonstrates for the first time the control over the structural ordering of anisotropic nanoparticles in a dynamic system using an electric field, which can have important implications for the development of sustainable alternatives to synthetic textiles.

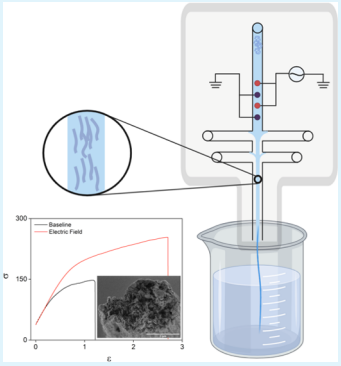

KEYWORDS: *nanofibrillated cellulose, nanoparticle orientation, flow focusing, electric field, renewable materials, mechanical properties*

INTRODUCTION

Cellulose nanofibrils (CNFs) are a class of earth-abundant biobased and biocompatible materials with attractive properties such as lightweight, thermal stability, and good strength.[1] When assembled into macroscale materials, the mechanical and dielectric performances of the resulting components are strongly influenced by the CNF orientation in these systems.[2,3] The development of highly ordered structures comprising cellulose-based nanomaterials with a high aspect ratio has recently spurred great interest.[4] In this context, multiple techniques for controlling the collective alignment of colloidal nanocellulose have been explored and can be divided into two categories depending on what type of external forces are used to impose alignment. Typical external forces involve mechanical stretching,[5−8] electric fields,[9−11] magnetic fields,[12−14] and liquid shear flow focusing,[15−19] while the tendency of certain particles to self-assemble into ordered structures can be exploited in some cases without the need for external forces.[20] Although electromagnetic applications have been widely used to align various elongated nanoparticles,[21−23] including cellulose nanocrystals,[10,24−26] studies focusing on nanofibrillated cellulose remain relatively scarce.[3,27] Among these methods, only the use of an AC electric field appears to be versatile enough for practical implementation. This is because the low magnetic susceptibility of cellulose requires unrealistically strong magnetic fields,[28] while the negative charges of CNF tend to generate aggregates at the anode when DC electric fields are applied.[29] When exposed to the AC electric field, individual CNFs rotate and align along the field direction if their movement is not restricted by the surrounding environment.[3] This is attributed to the anisotropic nature of the material, which ensures that the dipole moment in the direction parallel to the CNF main axis is stronger than the one in the perpendicular direction. After rotation, interfibril interactions take place to form cellulosic chains parallel to the electric field lines, which become thicker and longer as the electric field is applied for longer period of time. Some reports examined how the parameters of the applied electric field (i.e., amplitude, duration, etc.) influence the orientation of CNFs in various solutions,[3,27] while other researchers used a combination of shear forces and an electric field to improve nanocellulose alignment.[30] However, all these studies are limited to the preparation of thin films in batch experiments. To the best of our knowledge, there is no report in the literature where an AC electric field has been applied in a continuous flow system to control the nanoscale orientation of elongated particles.

Received: April 20, 2020
Accepted: May 26, 2020
Published: May 26, 2020

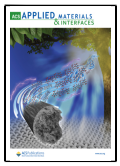

https://dx.doi.org/10.1021/acsami.0c07272

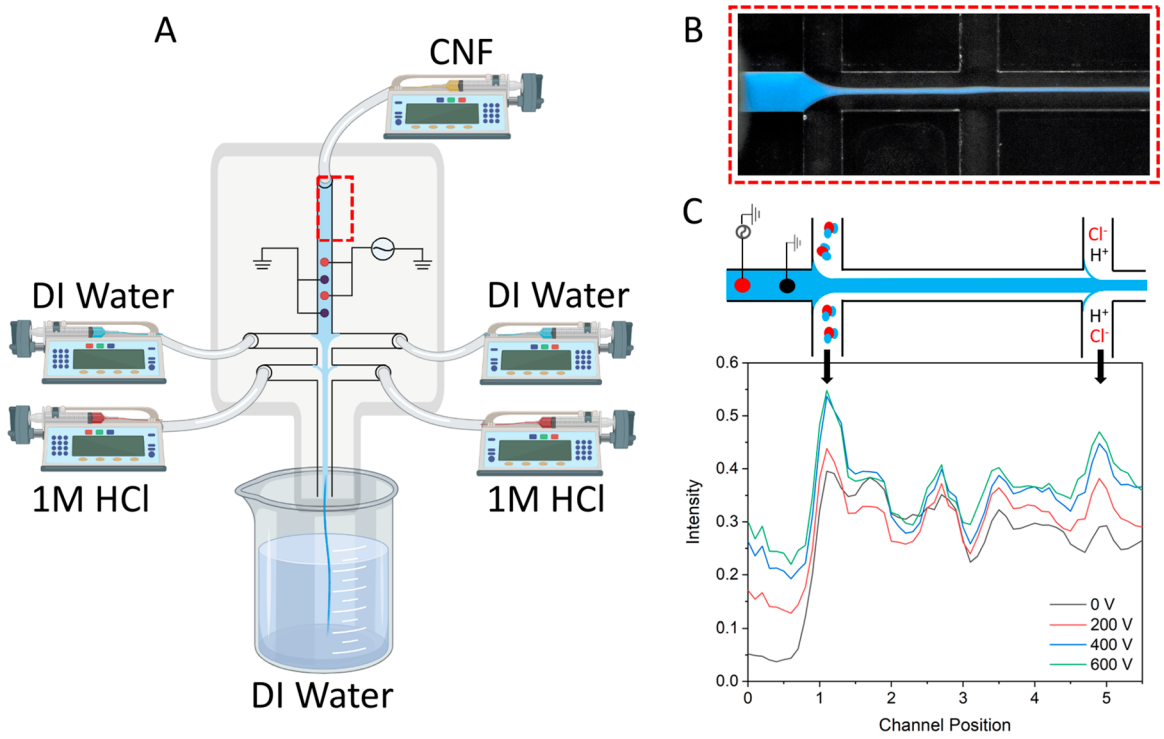

Figure 1. Assembly of nanostructured cellulosic filaments. (A) Schematic of the field-assisted double-flow-focusing channel used for the preparation of macroscopic filaments. The CNF suspension is injected in the core flow, while DI water and acid at low pH are supplied in the first and second extensional flows, respectively. (B) Optical microscope image of the double-flow-focusing part of the setup represented horizontally. Note that blue dyes were added to the core flow for clarity purposes. (C) Polarized optical transmission measurements of CNF alignment at various applied voltages along the core microfluidic channel, as illustrated in the above schematic.

One of the main challenges of using an AC external field in a dynamic process consists of locking the field-aligned CNFs into a metastable structure as the materials travel through the electric field to prevent the time dependent relaxation toward isotropy due to Brownian diffusion. Inspired by the flow-focusing approach,[31] the present study employs a set of extensional flows downstream to initiate a sol−gel transition before Brownian motion becomes dominant, hence forming highly ordered cellulose filaments. While the hydrodynamic alignment may induce nonuniform orientation profiles across the fiber width due to the inherent velocity gradient toward the channel walls,[32] the utilization of an AC electric field may help to mitigate this issue for the production of anisotropic and uniform fibers with larger diameters.

In this research, TEMPO-oxidized CNFs were extracted from renewable softwood pulp to produce anisotropic fibers using an innovative field-assisted flow-focusing process. The continuous production of renewable fibers with good mechanical attributes is particularly relevant considering that fibers account for more than 20% of the overall plastic production, which was valued at $55 trillion in 2017.[33] The evolution of CNF alignment during processing with regard to the applied voltage was studied *in situ* using polarized optical microscopy. Both surface and bulk order characterizations of the resulting filaments were conducted, respectively, by scanning electron microscopy coupled with image analysis and by orientation dependent variation of the polarized Raman scattering signal. 2D-XRD was performed to examine the CNF orientation in the planes perpendicular and parallel to the filament axis. Finally, several meters of filaments were produced under different conditions to investigate how the amplitude of the AC electric field influences the mechanical properties of the resulting nanocomposites.

RESULTS AND DISCUSSION

CNFs were synthesized on the basis of a previously reported TEMPO-mediated oxidation procedure with 3 mmol of NaClO per gram of bleached softwood pulp, followed by homogenization using mechanical blending and double acoustic irradiation.[34−37] As-prepared CNFs exhibited a mean length and diameter of 650 and 2 nm, respectively, yielding a high aspect ratio of 300 (Figure S1). Note that, for simplicity purposes, this value considers the fibers to be fully stretched out, which is unlikely to be the case in aqueous suspensions. The carboxylate content of CNFs was 0.7 mmol/g, as measured by conductometric titration (Figure S2), and the crystallinity index was 41%, as determined by XRD according to the Segal method (Figure S3).[38] The CNFs were completely dispersed at the individual nanofibril level in water by electrostatic repulsion and osmotic effects due to anionically charged carboxylate groups densely present onto the CNF surface.[39,40] Aqueous suspensions containing 0.3 wt % CNFs, exhibiting a viscosity of 13 mPa·s, were fed into a 1 mm microfluidic channel for the continuous fabrication of macroscopic cellulose filaments (Video S1). To align the CNFs in parallel with the filament axis, the core flow was equipped with 4 mm circular electrodes vertically spaced every 14 mm, with the electrode surface directly exposed to the CNF to generate an alternating AC electric field. Two extensional flows were installed downstream, with the first one composed of water and the second one comprising 1 M HCl, as illustrated in Figure 1A. A combination of five syringe pumps were used to

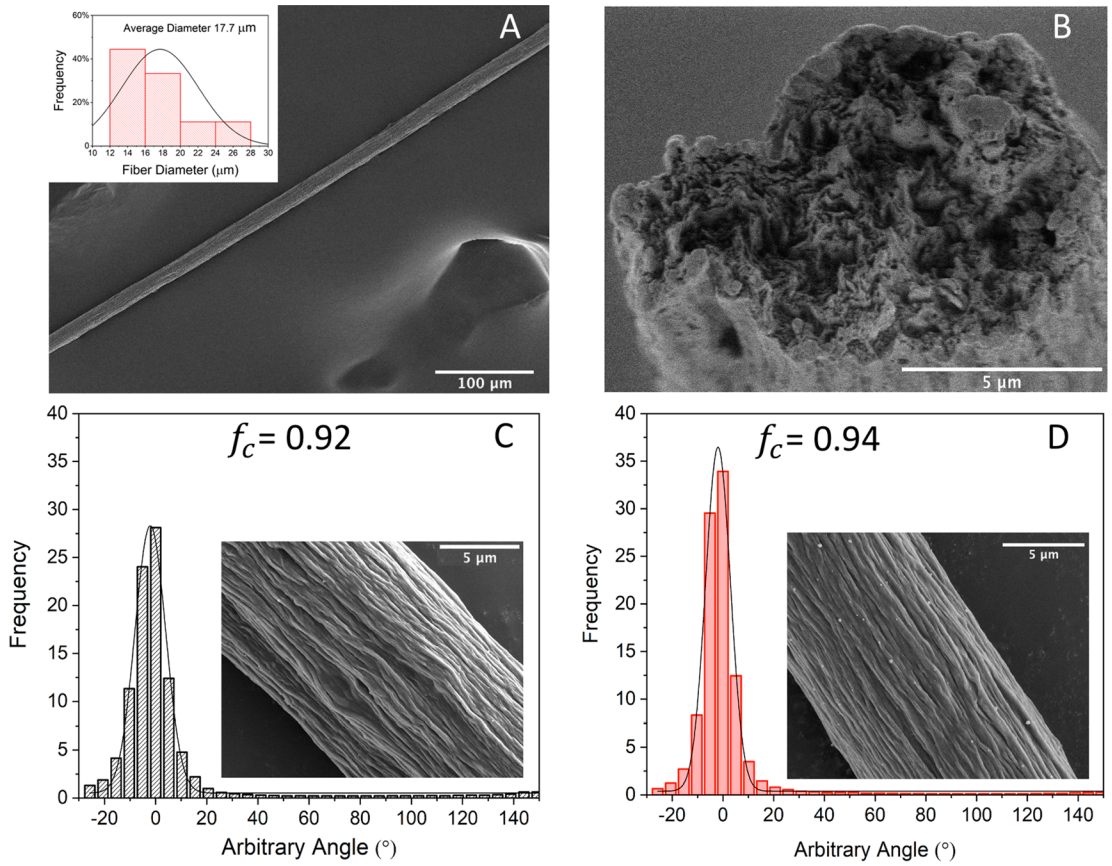

Figure 2. Morphological characterization of the prepared biobased filaments. (A) Representative SEM image of a cellulosic filament with the diameter distribution shown in the inset. (B) SEM image of the cross section of a filament showing a layered structure with dense CNF packing. Histograms representing the orientation degree of CNF threads on the surface of macroscopic filaments prepared (C) without and (D) with an external electric field. High magnification SEM images of the filament surfaces are shown in the insets.

control the flow rates of the core and all extensional flows, which were kept constant for all experiments. Optical transmission measurements of the core flow were collected between crossed polarizers to examine the birefringent properties of CNFs at different positions along the microfluidic channel. Experiments were conducted at different applied voltages varying from 0 to 600 V in 200 V increments. Voltages higher than 600 V were not considered to prevent water electrolysis. The variations in signal intensity observed at position 0 indicate that the sole electromagnetic polarization of the core flow gave rise to the nematic ordering of CNFs in solution, which gradually improved with increasing an applied AC external field. This means that the electrostatic torque exerted on the CNFs by the applied voltage was sufficient to overcome the effects of Brownian diffusion. It is also worth noting that the CNF response to the electric field was not linear and started to level off at elevated voltages, which is consistent with recent results from numerical simulations.[15] The magnitude of the field-assisted alignment at 600 V (i.e., signal intensity of 0.30) was only 25% lower than the nematic CNF ordering obtained by the extensional flows at position 1 when no voltage was applied (i.e., signal intensity of 0.37). This demonstrates that polar moieties grafted on the CNF surface during the TEMPO-mediated oxidation enable strong CNF polarization and spontaneous alignment of dipoles under an applied AC external field. In addition, the benefits of the field-assisted alignment are well maintained throughout the entire flow-focusing process despite Brownian diffusion. Besides assisting nanoparticle alignment by accelerating the core flow, the first set of extensional flows (i.e., position 1) generated a protecting sheath flow of DI water to prevent CNF friction with the microfluidic channel wall. When 600 V was applied compared to the baseline experiment without an AC external field, the signal intensity increased by 44% and 56% at the first and second extensional flow positions (i.e., channel positions 1 and 5), respectively. Beyond the second set of extensional flows (i.e., position 5), the presence of low pH acid limited electrostatic repulsions between individual CNFs due to the protonation of carboxyl (COO−) groups and promoted the sol−gel transition of the biopolymer, forming well-ordered macroscopic filaments.[31,41,42] These results reveal that the upstream field-assisted alignment of the core flow offers a unique opportunity to improve the downstream ordering of nanoparticles induced by extensional flows.

The continuous filaments made by the field-assisted flow-focusing process were cut into small sections and air-dried under tension for further characterization. Electron microscopy analysis revealed that all filaments exhibited similar ribbed textures with a mean diameter of 17.7 ± 4.3 μm regardless of the applied voltage (Figure 2A). The representative cross-section image of a filament in Figure 2B shows that CNFs were tightly packed into a well-defined layered structure. This was consistent with the XRD pattern of macroscopic filaments (Figure S3), which was similar to that of CNFs with a much lower intensity of cellulose peaks, suggesting a compact layout of CNFs. Observations at higher magnifications indicated that

each filament was composed of multiple CNF bundles of 1−3 μm in diameter forming aligned threads throughout the filament.[11] To assess the degree of alignment of these striations, the orientation index, f_c, was computed on the basis of eq S2 using ImageJ software.[43] This microscale orientation factor was determined for filaments prepared under the same flow conditions but at different applied voltages. The high ordering of CNF bundles was confirmed by orientation factors higher than 0.9 in each case. When an external electric field was applied (Figure 2D), the orientation index slightly increased from 0.92 to 0.94 compared to the baseline filament without applied voltage (Figure 2C). However, there were no statistically significant differences between the orientation factors measured at various applied voltages.

While the above results provided an estimate of the microscale directionality of CNFs on the external surface of the filament, polarized Raman spectroscopy was conducted at ambient conditions to better examine the bulk orientation and the quality of the alignment of individual CNFs within the filaments.[44,45] Samples were mounted on silicon dioxide wafers, and all spectra were collected at an excitation wavelength of 785 nm and normalized using the silicon dioxide signature peak at 521 cm^{-1}. The characteristic peak at 1095 cm^{-1}, commonly associated with the C−O vibration of the cellulose backbone parallel to the molecular chain axis,[46,47] was studied due to its strong dependence on the polarization angle.[48] Since the Raman intensity of randomly oriented fibrils remains constant regardless of the polarization angle, a systematic deviation from this can serve to characterize the degree of fibril alignment. Figure 3 shows that, when the long axis of the filament was parallel to the incident laser polarization (//), a large enhancement of the Raman intensity was observed for all specimens. Rotating the filaments from 0° to 90° reduced the intensity of the 1095 cm^{-1} band more dramatically for the filament prepared with the assistance of an external electric field. The filaments produced under applied voltage retained only 15.6% of their maximum intensity, while the filaments synthesized without an AC external field retained more than 30% of their maximum intensity. This significant change in intensity indicates that greater optical anisotropy was achieved when the applied voltage reached 600 V. Furthermore, the absence of shift in the main cellulose peaks revealed that the structural integrity of the filament was preserved under applied voltages up to 600 V (Figure S4). The combination of electron microscopy and image analysis with polarized Raman spectroscopy revealed that an externally applied electric field improved the alignment of CNFs both on the filament surface and in the bulk. In the absence of an AC electric field, however, bulk ordering was significantly reduced, while surface ordering was only slightly affected. This may be attributed to the radial velocity profile of CNFs from the core flow toward the channel walls.[32] Besides enhancing to some extent the magnitude of CNF ordering, the utilization of an AC electric field ensures a more uniform CNF orientation across the macroscale filament.

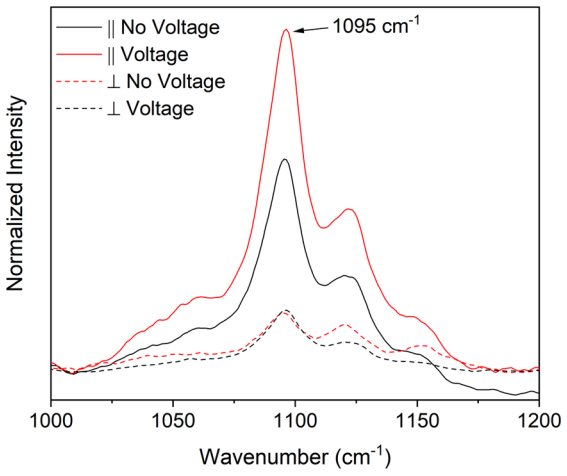

Figure 3. Raman spectra of cellulosic filaments prepared with (red) and without (black) an external electric field. The voltage applied in this case was 600 V. Each spectra was collected at an excitation wavelength of 785 nm in parallel with (solid line) and perpendicular to (dashed line) the filament axis.

To evaluate the influence of the amplitude of the electric field on the CNF ordering, filaments prepared at different applied voltages were characterized by 2D-XRD (Figure 4). The characteristic peak of the (200) crystallographic plane of cellulose at 2θ = 22.4°, commonly attributed to the d spacing between crystal regions of individual cellulose chains, was used to assess the CNF orientation in the filaments.[49,50] CNF orientation was analyzed both in the planes perpendicular (Ψ) and parallel (Φ) to the filament axis, as illustrated in Figure 4E. Parts A−D of Figure 4 report the evolution of the (200) band intensity as a function of the in-plane rotation angle for filaments produced under different conditions. Each specimen exhibited two distinct peaks at 0° and 180°, revealing the uniaxial orientation of CNFs along the filament axis. These peaks are obviously sharper in the case of the filaments prepared at 600 V, while only minimal variations of the peaks' full width half-maximum (fwhm) are observed for the other samples. This was consistent with the short appearance rate of the (200) band in the diffractogram of the 600 V filament compared to the other samples. The orientation index, f_c, was computed on the basis of eq S2 to quantify the quality of CNF alignment in the different filaments.[31,7] Note that the slight differences between the f_c values determined at 0° and 180° might be attributed to the difficulty of mounting perfectly stretched filaments onto the XRD stage. The averages between the f_c values calculated at 0° and 180° were considered for comparison purposes. The f_c values followed an upward trend and slightly increased from 0.815 to 0.865 when the applied voltage increased from 0 up to 400 V. Beyond this point, the f_c culminated to 0.945 at 600 V, representing a 16% increase from the baseline filament synthesized without an AC external field. These results reveal that, while the addition of an external electric field can improve CNF ordering, its effects become significant once a threshold voltage is applied to the core channel of the flow-focusing setup. This is consistent with previous batch experiments where no obvious alignment was observed in nanocellulose samples exposed to an electric field lower than a certain value.[24] In the out-of-plane direction (Figure 4F), however, the (200) band remained clearly visible in each diffractogram when the filaments were tilted from 0° to 90° without any obvious differences between filaments prepared at various applied voltages. This indicates the absence of preferential out-of-plane CNF orientation, suggesting that the CNFs were packed isotropically in-the-plane, Ψ, but parallel to the plane, Φ.

The influence of CNF orientation with respect to applied voltages on the mechanical response of the filaments was

https://dx.doi.org/10.1021/acsami.9b07373

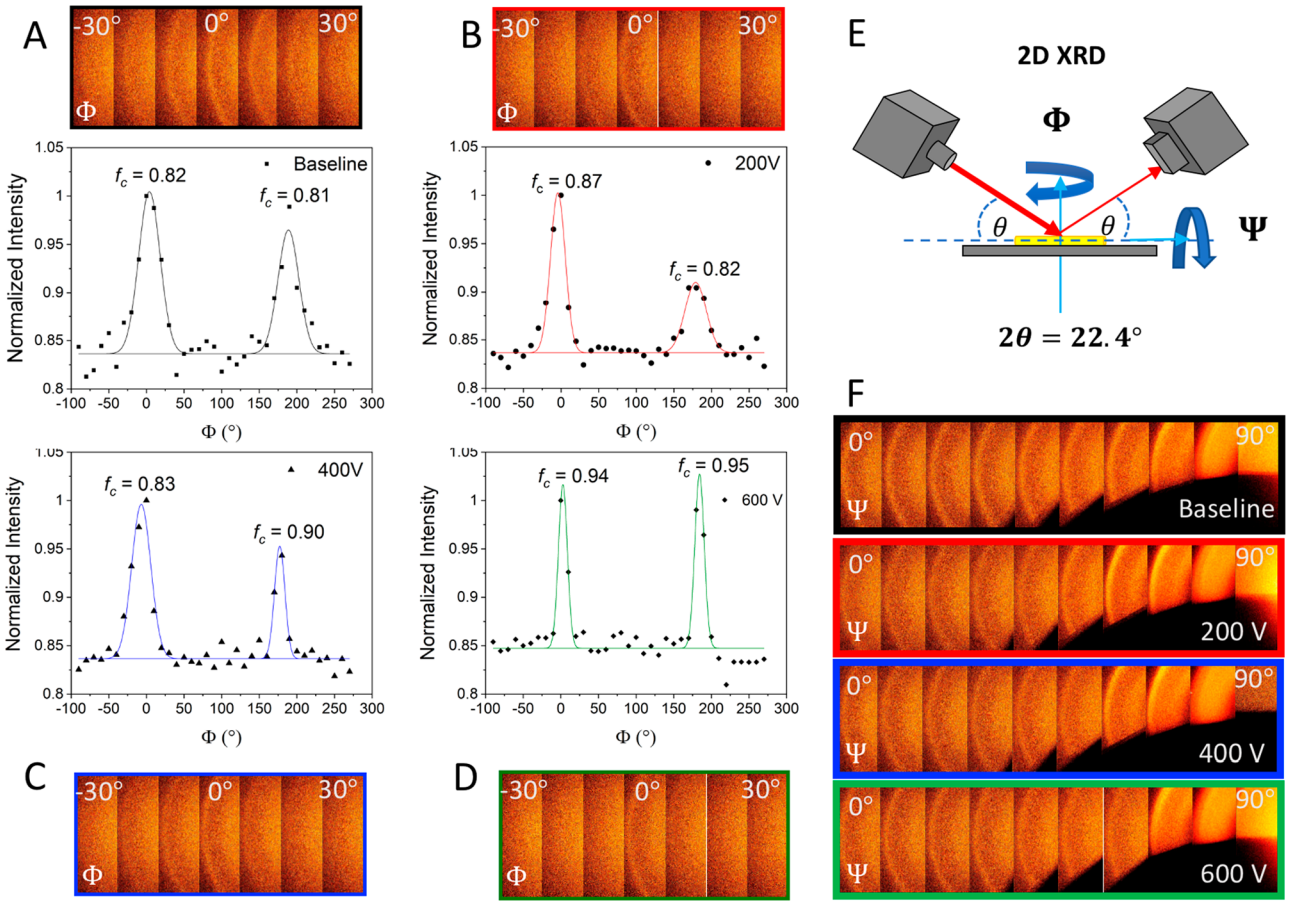

Figure 4. 2D XRD analysis of CNF alignment within the cellulosic filaments. (A) Azimuthal integration of the (200) scattering plane of the diffractograms with respect to Φ rotations for cellulosic filaments prepared at (A) 0, (B) 200, (C) 400, and (D) 600 V. (E) Schematic illustrating the axis of rotations with respect to the filament layout on the XRD stage for the in-plane, Φ, and out-of-plane, Ψ, directions. (F) Diffractograms of cellulosic filaments prepared at various applied voltages with respect to Ψ rotations.

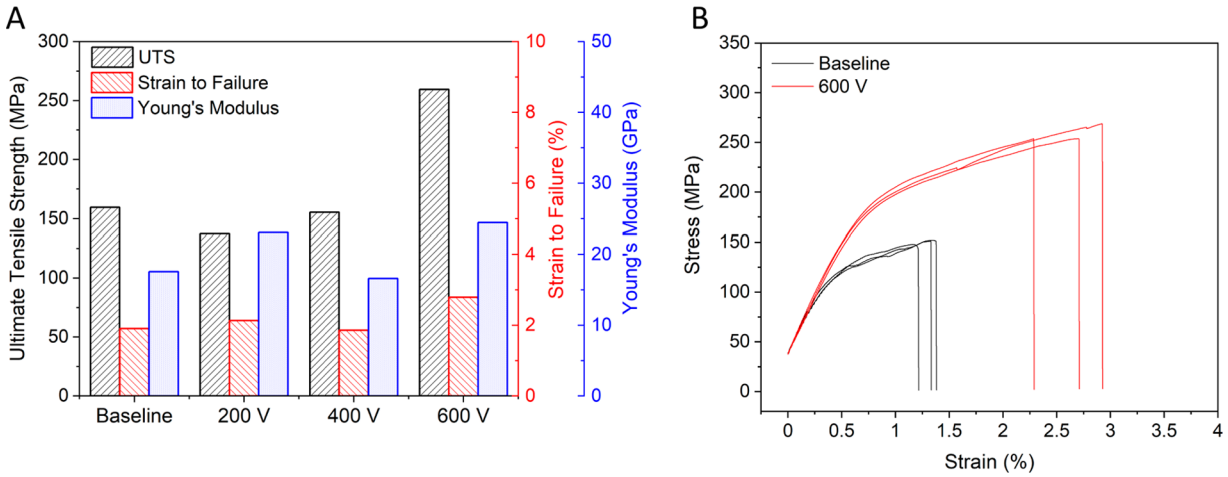

Figure 5. Mechanical properties of cellulosic filaments. (A) Bar graph showing the ultimate tensile strength, strain-to-failure, and Young's modulus of filaments prepared at different applied voltage. (B) Triplicate stress−strain curves of representative filaments prepared at 0 (black) and 600 V (red).

evaluated using stress−strain measurements. One meter long filaments were prepared at various applied voltages and were cut into 3 cm long sections. For statistical soundness, over 30 tensile tests were conducted for each condition and the results were subjected to one-way analysis of variance (ANOVA) and Tukey tests based on a 5% α level (i.e., 95% confidence). Statistical significance in tensile strength, strain-to-failure, and toughness were determined with p-values <0.05. As shown in Figure 5A, the tensile strength and strain-to-failure for the filaments prepared at 600 V were significantly larger than those for the others samples. This was consistent with the XRD data since the largest orientation enhancements were expected to

yield the greatest effects on the mechanical properties. Compared to the baseline filaments made without an electric field, the filaments at 600 V exhibited more than 63% and 46% augmentations in tensile strength and strain-to-failure, respectively. Such simultaneous increases in both tensile strength and strain-to-failure at 600 V yielded an impressive improvement of the material's toughness, with nearly 120% augmentation compared to the baseline filament prepared without an AC external field. It is noteworthy that this increase in toughness did not sacrifice the material's stiffness, as changes in the filaments' modulus of elasticity were not statistically significant. The Young's modulus hovered around 20 GPa, which is among the highest values reported for biobased materials.[32,51−53] In addition, the yield point, delineating the region when the material begins to deform plastically, was raised drastically when the applied voltage increased from 0 to 600 V, as depicted in Figure 5B. This reveals that important improvements in mechanical resilience can be achieved for structural materials with highly ordered nanofibrils. The good mechanical properties obtained at elevated voltages can be attributed to the anisotropic nature of the filaments combined with the tight CNF packing and limited electric field-induced structural defects.

CONCLUSION

In summary, macroscopic filaments comprising highly ordered TEMPO-oxidized CNFs were produced from renewable wood pulp using an innovative field-assisted flow-focusing process. Polar moieties on the CNF surface enabled strong polarization and spontaneous alignment of dipoles under an applied external electric field, which significantly improved the downstream nematic ordering of CNFs despite diffusion caused by Brownian motion. While the upstream field-assisted alignment enhanced the CNF ordering both on the filament surface and in the bulk, its effect became dominant once a threshold voltage was applied. Filaments produced at 600 V had greater optical anisotropy and exhibited a 16% augmentation in orientation index compared to filaments prepared without an AC external field. Despite the relatively high voltages that incurred, there were no signs of either electric field-induced structural defects or water electrolysis. 2D XRD analysis also revealed that the CNFs were randomly aligned in the plane along the filament length but oriented parallel to the filament axis. The high orientation degree of CNFs combined with their dense packing yielded impressive improvements in the mechanical properties of the resulting filaments, with up to 120% increase in toughness without compromising the material's stiffness. These results demonstrate for the first time that an external electric field can be applied in a continuous flow process to control the structural ordering of anisotropic materials. Future optimization of the biobased filaments can be made possible through the functionalization of CNFs with charged molecules and/or magnetic nanoparticles to tune the material response to an electromagnetic field and adjust interparticle interactions for multifunctional applications.

ASSOCIATED CONTENT

Supporting Information

The Supporting Information is available free of charge at https://pubs.acs.org/doi/10.1021/acsami.0c07272.

Discussions of CNF preparation and characterization, charge density of CNF dispersions, 2D X-ray diffraction, and fiber formation and characterization and figures of histograms, AFM images, plot of mixtures representing different aspects of the CNF synthetic process, intensity of films, and Raman spectroscopy (PDF)

Video of running microfluidic channel (AVI)

AUTHOR INFORMATION

Corresponding Author

Anthony B. Dichiara − *School of Environmental & Forest Sciences, University of Washington, Seattle 98195, United States;* orcid.org/0000-0002-3118-7029; Email: abdichia@uw.edu

Authors

Heather G. Wise − *School of Environmental & Forest Sciences, University of Washington, Seattle 98195, United States;* orcid.org/0000-0002-7627-1048

Hidemasa Takana − *Insititue of Fluid Science, Tohoku University, Sendai 980-8577, Japan*

Fumio Ohuchi − *Material Science & Engineering Department, University of Washington, Seattle 98195, United States*

Complete contact information is available at: https://pubs.acs.org/10.1021/acsami.0c07272

Notes

The authors declare no competing financial interest.

ACKNOWLEDGMENTS

This research was supported by the McIntire-Stennis Cooperative Forestry Research Program (grant# NI19MSCFRXXXG035, project accession# 1020630) from the USDA National Institute of Food and Agriculture and by the JSPS Kakenhi Program (grant# 19K04187). The present work was carried out under the University of Washington-Tohoku University: Academic Open Space and under the Collaborative Research Project of the Institute of Fluid Science, Tohoku University. The authors would like to acknowledge Mr. Ken Fukumori for his assistance with the filament preparation and Mr. Justin Niles for contributions to the cover art.

REFERENCES

(1) Tayeb, A. H.; Amini, E.; Ghasemi, S.; Tajvidi, M. Cellulose Nanomaterials—Binding Properties and Applications: A Review. *Molecules* **2018**, *23* (10), 2684.

(2) Mohammadi, P.; Toivonen, M. S.; Ikkala, O.; Wagermaier, W.; Linder, M. B. Aligning Cellulose Nanofibril Dispersions for Tougher Fibers. *Sci. Rep.* **2017**, *7* (1), 1−10.

(3) Kadimi, A.; Benhamou, K.; Ounaies, Z.; Magnin, A.; Dufresne, A.; Kaddami, H.; Raihane, M. Electric Field Alignment of Nanofibrillated Cellulose (NFC) in Silicone Oil: Impact on Electrical Properties. *ACS Appl. Mater. Interfaces* **2014**, *6* (12), 9418−9425.

(4) Zhu, Q.; Yao, Q.; Sun, J.; Chen, H.; Xu, W.; Liu, J.; Wang, Q. Stimuli Induced Cellulose Nanomaterials Alignment and Its Emerging Applications: A Review. *Carbohydr. Polym.* **2020**, *230*, 115609.

(5) Reising, A. B.; Moon, R. J.; Youngblood, J. P. Effect of Particle Alignment on Mechanical Properties of Neat Cellulose Nanocrystal Films. *Journal of Science & Technology for Forest Products and Processes* **2012**, *2* (6), 32−41.

(6) Fall, A. B.; Lindström, S. B.; Sprakel, J.; Wågberg, L. A Physical Cross-Linking Process of Cellulose Nanofibril Gels with Shear-Controlled Fibril Orientation. *Soft Matter* **2013**, *9* (6), 1852−1863.

(7) Tang, H.; Butchosa, N.; Zhou, Q. A Transparent, Hazy, and Strong Macroscopic Ribbon of Oriented Cellulose Nanofibrils Bearing Poly(Ethylene Glycol). *Adv. Mater.* **2015**, *27* (12), 2070−2076.
(8) Kafy, A.; Kim, H. C.; Zhai, L.; Kim, J. W.; Hai, L. V.; Kang, T. J.; kim, J. Cellulose Long Fibers Fabricated from Cellulose Nanofibers and Its Strong and Tough Characteristics. *Sci. Rep.* **2017**, *7*, 1.
(9) Kadimi, A.; Benhamou, K.; Habibi, Y.; Ounaies, Z.; Kaddami, H. Nanocellulose Alignment and Electrical Properties Improvement. In *Multifunctional Polymeric Nanocomposites Based on Cellulosic Reinforcements*; Puglia, D., Fortunati, E., Kenny, J. M., Eds.; William Andrew Publishing, 2016; pp 343−376. .
(10) Bordel, D.; Putaux, J.-L.; Heux, L. Orientation of Native Cellulose in an Electric Field. *Langmuir* **2006**, *22* (11), 4899−4901.
(11) Choi, K.; Gao, C. Y.; Nam, J. D.; Choi, H. J. Cellulose-Based Smart Fluids under Applied Electric Fields. *Materials* **2017**, *10* (9), 1060.
(12) Kim, H. C.; Kang, J.; Park, J. H.; Akther, A.; Kim, J. Feasibility Study of Cellulose Nanofiber Alignment by High DC Magnetic Field. *Nanosensors, Biosensors, Info-Tech Sensors and 3D Systems 2017*; International Society for Optics and Photonics, 2017; Vol. *10167*, p 101670H. .
(13) Sugiyama, J.; Chanzy, H.; Maret, G. Orientation of Cellulose Microcrystals by Strong Magnetic Fields. *Macromolecules* **1992**, *25* (16), 4232−4234.
(14) Pullawan, T.; Wilkinson, A. N.; Eichhorn, S. J. Influence of Magnetic Field Alignment of Cellulose Whiskers on the Mechanics of All-Cellulose Nanocomposites. *Biomacromolecules* **2012**, *13* (8), 2528−2536.
(15) Takana, H.; Guo, M. Numerical Simulation on Electrostatic Alignment Control of Cellulose Nano-Fibrils in Flow. *Nanotechnology* **2020**, *31*, 205602.
(16) Smith, D. E.; Babcock, H. P.; Chu, S. Single-Polymer Dynamics in Steady Shear Flow. *Science* **1999**, *283* (5408), 1724−1727.
(17) Lundahl, M. J.; Klar, V.; Wang, L.; Ago, M.; Rojas, O. J. Spinning of Cellulose Nanofibrils into Filaments: A Review. *Ind. Eng. Chem. Res.* **2017**, *56* (1), 8−19.
(18) Clemons, C. Nanocellulose in Spun Continuous Fibers: A Review and Future Outlook. *J. Renewable Mater.* **2016**, *4* (5), 327−339.
(19) Nechyporchuk, O.; Håkansson, K. M. O.; Gowda, V. K.; Lundell, F.; Hagström, B.; Köhnke, T. Continuous Assembly of Cellulose Nanofibrils and Nanocrystals into Strong Macrofibers through Microfluidic Spinning. *Advanced Materials Technologies* **2019**, *4* (2), 1800557.
(20) Mredha, M. T. I.; Le, H. H.; Tran, V. T.; Trtik, P.; Cui, J.; Jeon, I. Anisotropic Tough Multilayer Hydrogels with Programmable Orientation. *Mater. Horiz.* **2019**, *6* (7), 1504−1511.
(21) Gupta, P.; Rajput, M.; Singla, N.; Kumar, V.; Lahiri, D. Electric Field and Current Assisted Alignment of CNT inside Polymer Matrix and Its Effects on Electrical and Mechanical Properties. *Polymer* **2016**, *89*, 119−127.
(22) Oliva-Avilés, A. I.; Avilés, F.; Sosa, V.; Oliva, A. I.; Gamboa, F. Dynamics of Carbon Nanotube Alignment by Electric Fields. *Nanotechnology* **2012**, *23* (46), 465710.
(23) Chen, X. Q.; Saito, T.; Yamada, H.; Matsushige, K. Aligning Single-Wall Carbon Nanotubes with an Alternating-Current Electric Field. *Appl. Phys. Lett.* **2001**, *78* (23), 3714−3716.
(24) Habibi, Y.; Heim, T.; Douillard, R. AC Electric Field-Assisted Assembly and Alignment of Cellulose Nanocrystals. *J. Polym. Sci., Part B: Polym. Phys.* **2008**, *46* (14), 1430.
(25) Kalidindi, S.; Ounaies, Z.; Kaddami, H. Toward the Preparation of Nanocomposites with Oriented Fillers: Electric Field-Manipulation of Cellulose Whiskers in Silicone Oil. *Smart Mater. Struct.* **2010**, *19* (9), No. 094002.
(26) Aguié-Béghin, V.; Molinari, M.; Hambardzumyan, A.; Foulon, L.; Habibi, Y.; Heim, T.; Blossey, R.; Douillard, R. Preparation of Ordered Films of Cellulose Nanocrystals. *Model Cellulosic Surfaces*; ACS Symposium Series; American Chemical Society, 2009; Vol. *1019*, pp 115−136. .
(27) Xu, S.; Liu, D.; Zhang, Q.; Fu, Q. Electric Field-Induced Alignment of Nanofibrillated Cellulose in Thermoplastic Polyurethane Matrix. *Compos. Sci. Technol.* **2018**, *156*, 117−126.
(28) Tatsumi, M.; Kimura, F.; Kimura, T.; Teramoto, Y.; Nishio, Y. Anisotropic Polymer Composites Synthesized by Immobilizing Cellulose Nanocrystal Suspensions Specifically Oriented under Magnetic Fields. *Biomacromolecules* **2014**, *15* (12), 4579−4589.
(29) Ten, E.; Jiang, L.; Wolcott, M. P. Preparation and Properties of Aligned Poly(3-Hydroxybutyrate-Co-3-Hydroxyvalerate)/Cellulose Nanowhiskers Composites. *Carbohydr. Polym.* **2013**, *92* (1), 206−213.
(30) Csoka, L.; Hoeger, I. C.; Peralta, P.; Peszlen, I.; Rojas, O. J. Dielectrophoresis of Cellulose Nanocrystals and Alignment in Ultrathin Films by Electric Field-Assisted Shear Assembly. *J. Colloid Interface Sci.* **2011**, *363* (1), 206−212.
(31) Mittal, N.; Ansari, F.; Gowda, V. K.; Brouzet, C.; Chen, P.; Larsson, P. T.; Roth, S. V.; Lundell, F.; Wågberg, L.; Kotov, N. A.; Söderberg, L. D. Multiscale Control of Nanocellulose Assembly: Transferring Remarkable Nanoscale Fibril Mechanics to Macroscale Fibers. *ACS Nano* **2018**, *12* (7), 6378−6388.
(32) Håkansson, K. M. O.; Fall, A. B.; Lundell, F.; Yu, S.; Krywka, C.; Roth, S. V.; Santoro, G.; Kvick, M.; Prahl Wittberg, L.; Wågberg, L.; Söderberg, L. D. Hydrodynamic Alignment and Assembly of Nanofibrils Resulting in Strong Cellulose Filaments. *Nat. Commun.* **2014**, *5*, 4018.
(33) Lebreton, L. C. M.; van der Zwet, J.; Damsteeg, J.-W.; Slat, B.; Andrady, A.; Reisser, J. River Plastic Emissions to the World's Oceans. *Nat. Commun.* **2017**, *8* (1), 1−10.
(34) Goodman, S. M.; Ferguson, N.; Dichiara, A. B. Lignin-Assisted Double Acoustic Irradiation for Concentrated Aqueous Dispersions of Carbon Nanotubes. *RSC Adv.* **2017**, *7* (9), 5488−5496.
(35) Isogai, A.; Saito, T.; Fukuzumi, H. TEMPO-Oxidized Cellulose Nanofibers. *Nanoscale* **2011**, *3* (1), 71−85.
(36) Gu, J.; Hu, C.; Zhang, W.; Dichiara, A. B. Reagentless Preparation of Shape Memory Cellulose Nanofibril Aerogels Decorated with Pd Nanoparticles and Their Application in Dye Discoloration. *Appl. Catal., B* **2018**, *237*, 482−490.
(37) Rattaz, A.; Mishra, S. P.; Chabot, B.; Daneault, C. Cellulose Nanofibres by Sonocatalysed-TEMPO-Oxidation. *Cellulose* **2011**, *18* (3), 585.
(38) Segal, L.; Creely, J. J.; Martin, A. E.; Conrad, C. M. An Empirical Method for Estimating the Degree of Crystallinity of Native Cellulose Using the X-Ray Diffractometer. *Text. Res. J.* **1959**, *29* (10), 786−794.
(39) Fall, A. B.; Lindström, S. B.; Sundman, O.; Ödberg, L.; Wågberg, L. Colloidal Stability of Aqueous Nanofibrillated Cellulose Dispersions. *Langmuir* **2011**, *27* (18), 11332−11338.
(40) Gu, J.; Dichiara, A. Hybridization between Cellulose Nanofibrils and Faceted Silver Nanoparticles Used with Surface Enhanced Raman Scattering for Trace Dye Detection. *Int. J. Biol. Macromol.* **2020**, *143*, 85−92.
(41) Nishiyama, Y. Molecular Interactions in Nanocellulose Assembly. *Philos. Trans. R. Soc., A* **2018**, *376* (2112), 20170047.
(42) Nascimento, D. M.; Nunes, Y. L.; Figueirêdo, M. C. B.; de Azeredo, H. M. C.; Aouada, F. A.; Feitosa, J. P. A.; Rosa, M. F.; Dufresne, A. Nanocellulose Nanocomposite Hydrogels: Technological and Environmental Issues. *Green Chem.* **2018**, *20* (11), 2428−2448.
(43) Sydney Gladman, A.; Matsumoto, E. A.; Nuzzo, R. G.; Mahadevan, L.; Lewis, J. A. Biomimetic 4D Printing. *Nat. Mater.* **2016**, *15* (4), 413−418.
(44) Xu, Y.; Atrens, A. D.; Stokes, J. R. Liquid Crystal Hydroglass Formed via Phase Separation of Nanocellulose Colloidal Rods. *Soft Matter* **2019**, *15* (8), 1716−1720.
(45) Alizadehgiashi, M.; Khabibullin, A.; Li, Y.; Prince, E.; Abolhasani, M.; Kumacheva, E. Shear-Induced Alignment of

Anisotropic Nanoparticles in a Single-Droplet Oscillatory Microfluidic Platform. *Langmuir* **2018**, *34* (1), 322−330.
(46) Gierlinger, N.; Schwanninger, M.; Reinecke, A.; Burgert, I. Molecular Changes during Tensile Deformation of Single Wood Fibers Followed by Raman Microscopy. *Biomacromolecules* **2006**, *7* (7), 2077−2081.
(47) Wiley, J. H.; Atalla, R. H. Band Assignments in the Raman Spectra of Celluloses. *Carbohydr. Res.* **1987**, *160*, 113−129.
(48) Hsieh, Y.-C.; Yano, H.; Nogi, M.; Eichhorn, S. J. An Estimation of the Young's Modulus of Bacterial Cellulose Filaments. *Cellulose* **2008**, *15* (4), 507−513.
(49) Munier, P.; Gordeyeva, K.; Bergström, L.; Fall, A. B. Directional Freezing of Nanocellulose Dispersions Aligns the Rod-Like Particles and Produces Low-Density and Robust Particle Networks. *Biomacromolecules* **2016**, *17* (5), 1875−1881.
(50) Ureña-Benavides, E. E.; Kitchens, C. L. Wide-Angle X-Ray Diffraction of Cellulose Nanocrystal−Alginate Nanocomposite Fibers. *Macromolecules* **2011**, *44* (9), 3478−3484.
(51) Hooshmand, S.; Aitomäki, Y.; Norberg, N.; Mathew, A. P.; Oksman, K. Dry-Spun Single-Filament Fibers Comprising Solely Cellulose Nanofibers from Bioresidue. *ACS Appl. Mater. Interfaces* **2015**, *7* (23), 13022−13028.
(52) Henriksson, M.; Berglund, L. A.; Isaksson, P.; Lindström, T.; Nishino, T. Cellulose Nanopaper Structures of High Toughness. *Biomacromolecules* **2008**, *9* (6), 1579−1585.
(53) Galland, S.; Berthold, F.; Prakobna, K.; Berglund, L. A. Holocellulose Nanofibers of High Molar Mass and Small Diameter for High-Strength Nanopaper. *Biomacromolecules* **2015**, *16* (8), 2427−2435.